Oscillations in Rapid Fracture

Ariel Livne, Oded Ben-David, and Jay Fineberg
The Racah Institute of Physics, The Hebrew University of Jerusalem, Jerusalem 91904, Israel
(Received 6 September 2006; published 21 March 2007)

Experiments of pure tensile fracture in thin brittle gels reveal a new dynamic oscillatory instability whose onset occurs at a critical velocity, $V_C = 0.87C_S$, where C_S is the shear wave speed. Until V_C, crack dynamics are well described by linear elastic fracture mechanics (LEFM). These extreme speeds are obtained by suppression of the microbranching instability, which occurs when sample thicknesses are made comparable to the minimum microbranch width. The wavelength of these sinusoidal oscillations is independent of the sample dimensions, thereby suggesting that these macroscopic effects are due to an intrinsic microscopic scale that is unrelated to LEFM.

DOI: 10.1103/PhysRevLett.98.124301 PACS numbers: 46.50.+a, 62.20.Mk, 89.75.Kd

The dynamics of rapidly moving cracks are of both fundamental and practical importance. Driven by the elastic energy stored in a stressed body, brittle cracks accelerate towards their theoretical limiting speed [1] of the Rayleigh wave speed, V_R. However, in tensile fracture, the crack tip becomes unstable at less than half of V_R, sprouting small side cracks termed microbranches [2]. At this point, the single-crack state is replaced by a multicrack one and much of the energy flowing to the crack tip, is transformed into additional fracture surface. The density of microbranches increases with the main crack velocity and as a consequence, cracks are rarely observed at velocities greater than 0.6–$0.7V_R$.

We describe experiments performed on polyacrylamide gels. Fracture dynamics in these materials have been shown [3] to be identical to those of standard brittle amorphous materials, with the advantage that the extremely slow wave speeds in gels simplify the study of crack dynamics. We demonstrate that, when microbranches are suppressed, crack dynamics are well described by the single-crack equation of motion up to previously unattainable crack speeds. Surprisingly, we find that a new oscillatory instability occurs at a critical velocity close to V_R.

Our experiments were performed using sheets of brittle polyacrylamide gels of typical size $(X \times Y)$ 125×115 mm^2 and thickness $0.15 < d < 0.35$ mm where X, Y, and Z are, respectively, the propagation, loading, and sheet thickness directions. All experiments reported here were performed on polyacrylamide gels composed of 13.8% total monomer concentration and 2.6% bisacrylamide as cross linker [4]. Their measured shear modulus is $G = 35.2 \pm 1.4$ kPa yielding, for these neo-Hookean elastomers [3], a Young's modulus, $E = 3G = 106$ kPa and a shear (longitudinal) wave speed of $C_S = 5.90 \pm 0.15$ m/s ($C_L = 11.8 \pm 0.3$ m/s) [5]. Measurements of C_S and C_L using high-speed photography agree with these values to within 0.1 m/s. Experiments using other gel compositions (e.g., 23% total monomer concentration with 10% bisacrylamide whose $C_S \sim 17$ m/s) exhibit similar qualitative and quantitative behavior. The gels were cast for each experiment between flat glass plates. To ensure uniformity, the evaporation of the gel's water content was limited to below 5%. We compensated for any resulting variations in wave speeds by direct measurement of G for each experiment.

The experimental setup and measurement techniques are described elsewhere [3]. The gel sheets were loaded in mode I (uniaxial extension) via constant displacement in the vertical (Y) direction. When a desired stress was reached, a shortcut was made at the sample's edge, midway between the vertical boundaries. This seed crack either immediately or after a short creep accelerated to dynamic velocities. The crack tip's instantaneous location was monitored by a high-speed camera set to a $X \times Y$ spatial resolution of $1280 \times 64/96$ pixels (frame rate of 7.2/5 kHz). The resulting fracture surface (XZ plane) was analyzed via an optical microscope and the fracture profile (XY plane) was scanned with 2400 dpi resolution.

The dynamics of a typical experiment on thin gels are presented in Fig. 1(a). The initial crack propagates along a straight trajectory until losing its directional stability to crack tip oscillations in the XY plane. Straight-line propa-

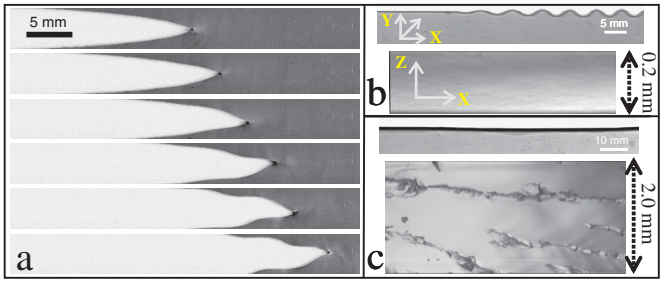

FIG. 1 (color online). (a) A sequence of photographs, shown at 0.69 ms intervals, of a propagating crack undergoing a transition from linear (top two pictures) to oscillatory motion. Photographs of XY profile (top) and (XZ) fracture surface (bottom) of (b) a 0.2 mm thick gel sample where oscillations developed and (c) a 2.0 mm thick gel where the crack retained its straight-line trajectory. In (c) the fracture surface is microbranch dominated, whereas in (b) the oscillating crack has a mirror surface. Propagation in (a), (b), and (c) was from left to right.

gation [Fig. 1(b)] typical of microbranch free fracture gives way to sinusoidal oscillations at a millimeter scale. The fracture surface formed by oscillating cracks is typically smooth (mirrorlike), with rare instances of short directed lines of successive microbranches ("branch lines") [6]. This behavior is in contrast to propagation in thicker samples where the crack retains its straight-line trajectory [Fig. 1(c)] while the fracture process is microbranch dominated; beyond a critical velocity branch lines develop whose density increases with the crack velocity [6]. Branch lines disappear upon arrival at the sample surfaces at $Z = 0$ or $Z = d$. Thus, in thin sheets branch lines are quickly suppressed and sporadic.

The onset of the oscillations occurs at a critical velocity [Fig. 2(a)] of $V_C = (0.87 \pm 0.02)C_S$ (with $V_C \sim 0.9C_S$ for gel compositions where $C_S \sim 17$ m/s). V_C is independent of d for $0.15 < d < 0.3$ mm. In thicker gels, cracks rarely reached V_C due to microbranching. Surprisingly, no evidence of the Yoffe instability [7], in which a crack is expected to deviate from its original straight-line trajectory at $V > 0.6V_R$, is observed.

The rapid acceleration to the extreme crack velocities attained ($V > 0.87C_S$) suggests that waves reflected from the system's remote boundaries cannot affect crack dynamics, as reflected waves only catch up with the crack tip well beyond the crack length $l = l_c$, where $V = V_C$. Thus, for $V \leq V_C$, predictions by linear elastic fracture mechanics (LEFM) [1] of the equation of motion, $V = V_R[1 - \Gamma(V)E/K^2]$, for a single edge crack in a semi-infinite body for which $K = 1.12\sigma\sqrt{\pi l}$ [8], should hold. Here Γ is the material's fracture energy. At $V = V_C$ this predicts l_c to be

$$l_c = \frac{\Gamma(V_C)E}{1.12^2\pi\sigma^2(1 - V_C/V_R)}. \quad (1)$$

Equation (1) predicts that $l_c \propto \sigma^{-2}$ where σ is the applied stress. This prediction [Fig. 2(b)] is, indeed, in excellent agreement with measurements of l_c. The slope of the linear fit yields a value of the fracture energy, $\Gamma(V_C) = 34 \pm 9$ J/m^2, which agrees with previous measurements [9]. The slight scatter in Fig. 2(b) is consistent with our 5% allowed variation of G.

At V_C the behavior of the crack's velocity components V_x and V_y changes abruptly. Prior to V_C, $V_y = 0$ whereas beyond V_C, V_y oscillates at a wavelength $\lambda(x)$ with increasing amplitude. The oscillations in V_y are accompanied by a much smaller oscillatory component of V_x having a wavelength of $\lambda/2$ and a $\pi/2$ relative phase shift. [Fig. 2(a) inset]. This suggests that $V = \sqrt{V_x^2 + V_y^2}$ does not, itself, oscillate but increases monotonically, although we lack the temporal resolution to directly verify this.

While V_x increases until reaching V_C, after the instability onset its mean value over an oscillation period unexpectedly remains nearly constant (even dropping by a few percent). Beyond V_C, however, V generally continues to accelerate (see, e.g., Fig. 3) to steady-state velocities, but does not surpass C_S [10]. This effect is illustrated in Fig. 3 (inset) where, assuming that V_x is constant [11], V obtained by integrating the measured path length of the crack is identical to measured values for $V > V_C$.

Let us consider the nature of the oscillations. The oscillations are generally sinusoidal except for large amplitude states at the highest values of applied stress σ. Both the oscillation amplitude A and wavelength λ develop with crack advance until reaching steady-state values after a number of cycles (Fig. 4 insets). The steady-state values of both A and λ vary with σ, as shown in Fig. 4, and do not appear to be well-defined functions of V. At $V = V_C$, A initiates from a finite value, although no hysteresis in the transition to the oscillatory state has been observed. λ is a sharply decreasing function of σ. Steady-state wavelengths

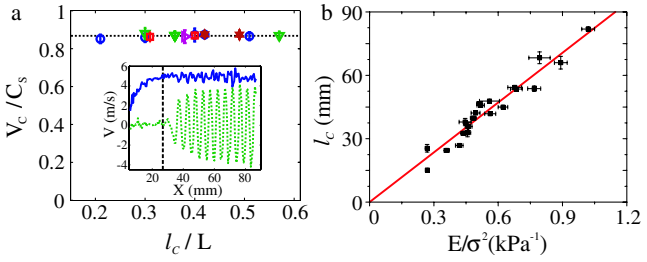

FIG. 2 (color online). (a) Oscillations appear only beyond a critical velocity of $V_C = 0.87C_S$ (dashed line). V_C is independent of the crack length at the onset l_c, sample size L, thickness d, and applied stress σ. The different symbols represent measurements for $0.15 < d < 0.30$ mm. (inset) V_x (continuous line) and V_y (dotted line), as a function of X. (b) The measured (squares) and predicted (line) relation between l_c and E/σ^2 in the framework of LEFM [1]. The line's slope gives the fracture energy $\Gamma(V_C) = 34 \pm 9$ J/m^2.

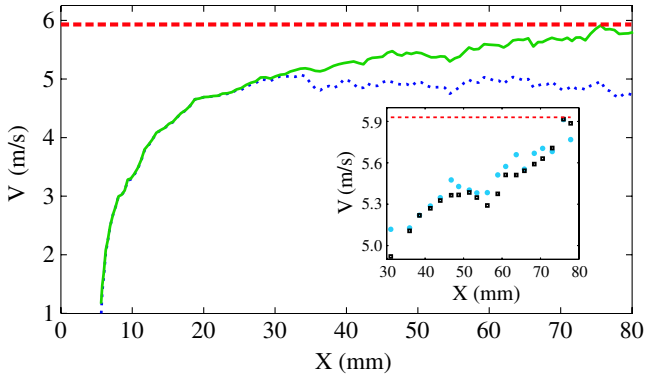

FIG. 3 (color online). The full crack velocity V (continuous line), is compared to V_x (dotted line). Beyond V_C, V increases until C_S (dashed line) [10], while V_x stays nearly constant. (inset) A comparison of direct measurements of V beyond V_C (full circles) with V, calculated using the spatial trajectory of the oscillations (squares) [11]. The dashed line denotes C_S. All velocities are averaged over an oscillation period.

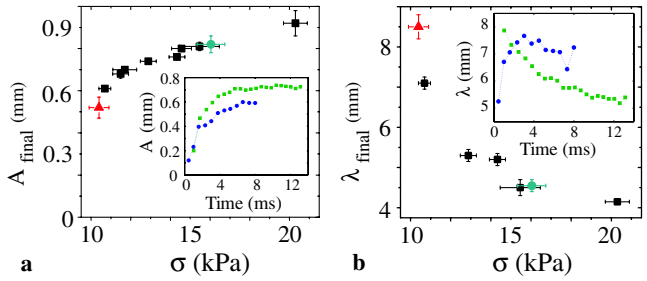

FIG. 4 (color online). Steady-state amplitudes A (a) and wavelengths λ (b) as a function of the applied stress σ. (insets) Transient time evolution of A and λ in two typical experiments. $t = 0$ defines the onset of oscillations. Sample dimensions: $(X \times Y) \sim 125 \times 115$ mm^2 (■), 130×155 mm^2 (▲), and 125×70 mm^2 (●).

range from 4–9 mm with $V_x/\lambda \sim 0.5$–1 kHz. This frequency scale corresponds to the same (~1 ms) time scale that was previously observed for microbranching activation times in similar gels [3]. The origin of these length and time scales is currently unknown. The time scale is notably less than viscoelastic time scales and over an order of magnitude smaller than any resonance with the system's boundaries. In fact, these scales are wholly independent of any of the physical dimensions of the sample, since gels of substantially different widths and dimensions all fall on the same steady-state amplitude and wavelength curve (Fig. 4). Furthermore, as indicated by Fig. 2(b), the crack is effectively traveling in a semi-infinite medium at the onset of oscillations and, under semi-infinite conditions, the crack will have no knowledge of the actual size of the sample. We surmise that this length scale has its origins in an intrinsic scale, such as the process zone, that is not quantitatively accounted for in current theoretical frameworks.

Although the steady-state values of λ and A are well defined, their initial transients (Fig. 4, insets) are extremely diverse, with no discernible relation to either V or σ. It is interesting, however, that these transients follow a number of distinct A-λ trajectories, suggesting that there may be a number of metastable solution branches that eventually evolve to the steady states presented in Fig. 4.

Why is the oscillatory instability not readily observed in thick samples? Basically, in thick samples cracks rarely attain V_C, due to the onset of microbranching. Let us momentarily digress and consider the relation of microbranch formation to sample thickness. Recent work in gels indicates that the microbranching instability is a first-order phase transition in which microbranch formation is triggered by noise, above a critical velocity [3]. Microbranches in gels have a minimal width [3], ΔZ, whose scale (here ~40 μm) is near the process zone size, as estimated by $\Gamma E/(2\pi\sigma_y^2) \sim 50$ μm (in these gels the yield stress $\sigma_y \sim E$ [12]). The system's quenched noise level may then be related to $d/\Delta Z$. This may explain why the number of branching events is strongly suppressed with decreasing d. This suppression, coupled with the disappearance of branch lines with their arrival at the sample faces at $Z = 0$ or d [see, e.g., Fig. 1(c)], causes the increasingly sporadic appearance of microbranches as $d \to \Delta Z$. Thus for $d \to \Delta Z$ ($\Delta Z \sim \mu$m for poly-methyl-methacrylate and less for glass) microbranching events are rare with crack dynamics becoming effectively two dimensional. This suppression of microbranches explains how oscillations are so readily obtained for $d \sim 0.15$–0.2 mm.

Although rare, the microbranching instability is observed in thin sheets both in straight and oscillatory propagation. When excited, microbranches reduce the energy available to the main crack [2], and consequently reduce the main crack's velocity. If V falls below V_C, oscillations immediately cease, and the crack propagates along a straight trajectory (e.g., Fig. 5 in the second shaded region). When microbranching is sporadic, microbranches only momentarily reduce V to below V_C. This not only causes discontinuities in the oscillation phase but before and after a velocity drop we often observe entirely different sinusoidal solutions (with significantly different wavelength and amplitude). When prolonged microbranching occurs, as characteristic of the thicker gels, V only momentarily surpasses V_C between microbranching events. In this case, pronounced "staircase" profiles are created by momentary deviations of the crack for less than a period followed by straight-line trajectories. All of these effects are demonstrated in the single experiment, presented in Fig. 5, in which d is tapered as a function of X. The rarity of

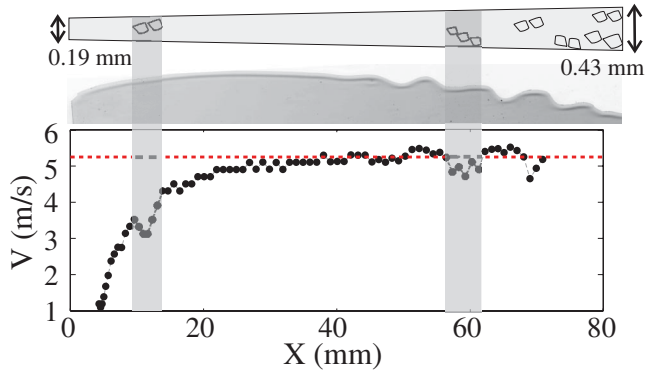

FIG. 5 (color online). Tapering of d ($0.19 < d < 0.43$ mm) as a function of X enables $V > V_C$ for thicknesses ($d > 0.35$ mm) normally dominated by microbranches. (top) Schematic drawing of the XZ fracture surface indicating branch line locations and $d(x)$. (center) Photograph of the crack profile along the XY plane with (bottom) the corresponding velocity profile. Shaded rectangles indicate regions of sporadic branch lines (diamonds at top) and the resulting drops in V until their disappearance when a branch line encounters the $Z = 0$ or d planes. When $V < V_C$ (V_C denoted by the dashed line) oscillations cease with no hysteresis and cracks continue along a straight-line trajectory (e.g., second shaded region). Prolonged branching ($d > 0.35$ mm) yields staircase profiles.

microbranches in the initial stage ($d < 0.35$ mm) enables rapid acceleration to $V > V_C$ and the onset of oscillations. As the taper widens, microbranching occurs; first sporadically (2nd shaded region) and later with prolonged branching (for $d > 0.35$ mm), leading to staircase profiles.

In recent years, two oscillatory instabilities of cracks traveling in thin sheets have been reported. Both of these are fundamentally different from the oscillatory instability presented here. Deegan and coworkers have observed wavy cracks traveling at intersonic velocities in biaxially stretched thin rubber sheets [13]. In our experiments, oscillations are observed at clearly subsonic velocities in pure uniaxial tension. Phase field models [14], which do yield subsonic oscillations of crack trajectories, predict λ to scale with the system size, also in sharp contrast with our results. Recent calculations [15], pairing LEFM with the Hodgdon and Sethna [16] path selection criterion, predict the onset of oscillatory instability at close to our measured values of V_C. In contrast to our measurements, however, λ is predicted to scale with the system size.

Oscillatory cracks have also been observed when a rigid cutting tool is forced through a thin elastic sheet [17]. These cracks travel at $V \ll C_S$ with out-of-plane bending playing an important role. In contrast, the instability presented here is in pure mode I with no measurable out-of-plane deflection [18] and with V_C values that are near C_S. In addition, the crack dynamics in our experiments are consistent with the single-crack (mode I) equation of motion predicted by LEFM until either V_C or the onset of microbranching.

Our experiments indicate a newly identified intrinsic instability in dynamic fracture whose characteristic length/time suggests that a new scale is needed to describe these dynamics. Although leading to macroscopic behavior, this scale must be microscopic (e.g., the process zone), as it is not included within LEFM [15]. The instability's existence underlines the necessity for a more fundamental understanding of the near vicinity of the crack tip and highlights important unresolved questions regarding both the path selection of dynamic cracks [16,19] and how this is influenced by near-tip dynamics. Furthermore, microbranch suppression when gel thicknesses approach the process zone scale, raises interesting questions regarding both the origin of the microbranching instability and the relevant length scales at which 3D fracture becomes effectively 2D.

We thank the Israel Science Foundation for support.

[1] L. B. Freund, *Dynamic Fracture Mechanics* (Cambridge University Press, Cambridge, 1990).

[2] E. Sharon and J. Fineberg, Phys. Rev. B **54**, 7128 (1996).

[3] A. Livne, G. Cohen, and J. Fineberg, Phys. Rev. Lett. **94**, 224301 (2005).

[4] The acrylamide solution contains weight/vol 0.02% of NaCl and ~60 ppm bromophenol blue to facilitate visualization. Polymerization is initiated by adding 0.12% APS and 0.06% TEMED.

[5] Expressions for C_S and C_L for 3D neo-Hookean elastomers were obtained by generalizing Petersan *et al.* [14]. In the material reference frame $C_S = (G/\rho)^{1/2}$ while, in the x direction, $C_L = 2C_S$.

[6] E. Sharon, G. Cohen, and J. Fineberg, Phys. Rev. Lett. **88**, 085503 (2002).

[7] E. H. Yoffe, Philos. Mag. **42**, 739 (1951).

[8] B. Lawn, *Fracture of Brittle Solids* (Cambridge University Press, Cambridge, 1993), 2nd ed.

[9] Y. Tanaka, K. Fukao, and Y. Miyamoto, Eur. Phys. J. E **3**, 395 (2000); T. Baumberger, C. Caroli, and D. Martina, Nat. Mater. **5**, 552 (2006).

[10] The limiting velocity should be $V_R = 0.955C_S$ and not C_S. In a number of experiments, the crack's maximal velocity was between V_R and C_S. This discrepancy might be due to measurement accuracy (~3%) or a different form for V_R in elastomers or thin sheets.

[11] From postmortem XY scans of the gels, we measure λ and A for each period. The corresponding length of the crack's path is $l = \lambda F(A/\lambda)$. Defining $\bar{V}$ and $\bar{V}_x$ as the mean values of V and V_x over one period (T) we find $\bar{V} = l/T$ and $\bar{V}_x = \lambda/T$. Therefore $\bar{V}/\bar{V}_x = F(A/\lambda)$ where F is solved numerically.

[12] J. Zhang, C. R. Daubert, and E. A. Foegeding, Rheol. Acta **44**, 622 (2005).

[13] R. D. Deegan, P. J. Petersan, M. Marder, and H. L. Swinney, Phys. Rev. Lett. **88**, 014304 (2001); P. J. Petersan, R. D. Deegan, M. Marder, and H. L. Swinney, Phys. Rev. Lett. **93**, 015504 (2004).

[14] H. Henry and H. Levine, Phys. Rev. Lett. **93**, 105504 (2004); A. Karma and A. E. Lobkovsky, Phys. Rev. Lett. **92**, 245510 (2004).

[15] E. Bouchbinder and I. Procaccia, following Letter, Phys. Rev. Lett. **98**, 124302 (2007).

[16] J. A. Hodgdon and J. P. Sethna, Phys. Rev. B **47**, 4831 (1993).

[17] A. Ghatak and L. Mahadevan, Phys. Rev. Lett. **91**, 215507 (2003); B. Roman *et al.*, C. R. Mécanique **331**, 811 (2003).

[18] Mode III fracture was ruled out by the following: a thin laser sheet, oriented at 30° to the gel plane and parallel to the Y axis, illuminated a line upon the gel where future crack oscillations appear. When traversed by the crack, no deflection of the line was observed, thus indicating a $<5°$ mode III component.

[19] M. Marder, Europhys. Lett. **66**, 364 (2004); G. E. Oleaga, J. Mech. Phys. Solids **49**, 2273 (2001).